# PERFORMANCE OF MODIFIED BASALT FIBRES

T. Förster*, E. Mäder
Dept. Composite Materials, Leibniz-Institut für Polymerforschung Dresden e.V. (Leibniz Institute of Polymer Research), Dresden, Germany
* Corresponding author (foerster-theresa@ipfdd.de)

**Keywords**: *basalt fibres, single fibre tensile strength, Weibull distribution, durability*

## 1 Introduction

Current research tasks focus on basalt fibres as new successful reinforcement fibres for different kinds of composites. Basalt fibre properties have been discussed as superior compared with fibre properties of commonly utilized E-glass fibres. Especially, mechanical, thermal and chemical properties are often promoted by basalt fibres manufactures. It is well known, that basalt is generated by rapid cooling of lava at earth's surface. This is the reason for an extensive availability of basalt rocks and the thought of an exhaustless raw material source, which seems to be a very attractive economic aspect for fibrization.

In this work, the chemical composition of basalt is modified by adding $Al_2O_3$, MgO and $TiO_2$ in order to increase the mechanical performance and the alkali resistance. Mechanical performance of basalt fibres is investigated by single fibre tensile tests and analysed by Weibull distribution. Both model fibres and commercial basalt fibres are analyzed. Alkali resistance of model basalt fibres is evaluated by accelerated ageing in alkaline media.

## 2 Experimental

### 2.1 Materials

Model basalt fibres in the unsized state (MOD1-5, Fig. 1) were made by using a lab-scale equipment. The raw materials of these model fibres were ground and partly blended with additives, namely $TiO_2$, MgO and $Al_2O_3$. Only small amounts of additives (up to 5 wt%) were added to the batches in order to keep the character of a basaltic composition. The range of some typical compositions of basalts for fibrization is about 49-57 wt% $RO_2$, 22-31 wt% $R_2O_3$ and 15-26 wt% $RO+R_2O$ [1].

MOD1 and MOD2 are model fibres out of natural basalt rocks. In contrast to MOD2, MOD1 is rich in oxides of type $RO_2$, like $SiO_2$ and $TiO_2$, and poor in oxides of type RO and $R_2O$, like CaO, MgO, $Na_2O$ and $K_2O$ (Fig. 1).

Commercial fibres (COM1-6) were provided by different manufacturers.

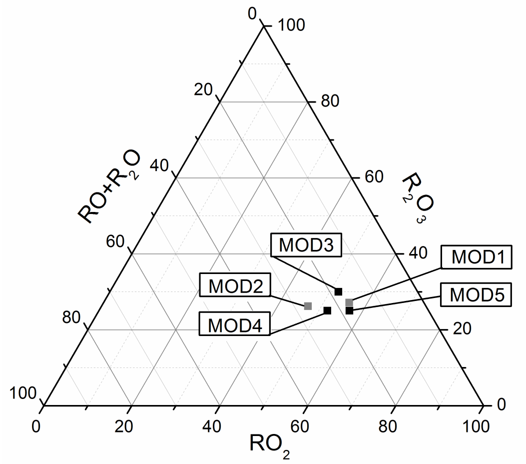


Fig. 1. Ratio of major constituents of basalt fibres. MOD1 and MOD2 are compositions of natural basalt rock resorts, MOD3 - MOD5 contain additives.

### 2.2 Methods

*Single fibre tensile test*

Single fibre tensile tests were conducted under air-conditioning (temperature 23°C, rel. humidity 50 %) by using a Favigraph semi-automatic testing device (Textechno, Mönchengladbach, Germany) equipped with a 1 N load cell. The cross head velocity was 25 mm/min and the gauge length was 50 mm. The fineness of each selected fibre was determined by using the vibroscope method in accordance with ASTM D 1577. 50 single fibres were tested for the determination of the average strength of commercial basalt fibres COM1-6, whereas up to 150 values were averaged for model basalt fibres MOD1-5, because of the higher scatter of the lab-materials.

*Weibull analysis*

The tensile test results were evaluated by Weibull probability analysis according to equation 1. The method is described in detail elsewhere [2].

$$P(\sigma) = 1 - e^{-\left(\frac{\sigma}{\sigma_0}\right)^m} \qquad (1)$$

The scale parameter $\sigma_o$ represents the stress at which 63.2 % of the filaments break ($P(\sigma_o)$=0.6321). The shape parameter *m* designates the Weibull modulus and is a measure of the distribution of the failure stress. A higher value of *m* indicates that the filaments fail in a narrow range of failure stresses. The Weibull parameters are determined by plotting ln(-ln(1-P) against ln(σ) (Fig. 2). Thereby, *m* is equal to slope of the generated curve and $\sigma_0$ is taken from x-value of interception with ln(-ln(1-P) = 0.

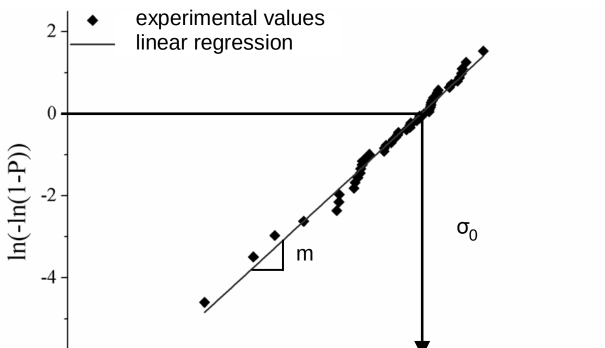


Fig. 2. Weibull probability plot and determination of Weibull parameter $\sigma_o$ and *m*.

*Estimation of modulus value*

Moduli of fibres at a strain range of 0-0,5 % were determined by single fibre tensile tests at different gauge lengths (20, 35, 50 and 80 mm).

The results are influenced by the clamp equipment leading in a dependence of modulus on gauge length. Liu [2] showed two different approaches to correct this effect.

Generally, the influence of the clamps becomes less important with increasing gauge length.

In this work, the Young's modulus was estimated by equation 2.

$$E_m = E_f + \frac{C}{l_{fo}} \qquad (2)$$

where $E_m$ is the measured modulus value, $E_f$ is the calculated modulus value, $l_{fo}$ is the gauge length of fibre and *C* is a constant. *C* was determined by fitting equation 2 in the plot of $E_m$ against $l_{fo}$.

*Alkali treatment*

The model basalt fibres (MOD1-5) were stored in 3-ionic solution at a temperature of 40°C for 7, 14, and 28 days. The 3-ionic solution consists of 1g/l NaOH, 4g/l KOH, 0,5g/l $Ca(OH)_2$.

For accelerated ageing the fibres also have been stored in 5 wt% sodium hydroxide solution at 80°C for 1, 2, 4 , 7 and 11 days. After ageing the fibres were embedded in epoxy resin in order to prepare polished cross sections.

*Characterization of the corrosion progress*

Before and after ageing in 3-ionic solution the tensile strength was determined by single fibre tensile test. In our previous work [3] we could show that Weibull distribution is a tool for the indirect detection of corrosion progress on fibre surfaces. For example, a typical behaviour for ageing in NaOH solution is that the failure stress steadily decreases, being interrupted by phases of increasing stresses. This effect was accompanied by formation of a peeling shell. In this work, a method was applied to characterize corrosion process in 3-ionic solution.

Furthermore, the initial state and the ageing progress in NaOH solution were evaluated by determining the fibre diameter by optical microscopy (Keyence Deutschland GmbH) as well as SEM images of the cross sections using a Scanning Electron Microscope (SEM) Ultra Plus (Zeiss, Germany). The specimens were sputter-coated with platinum.

## 3 Results and Discussion

### 3.1 Mechanical performance

Tab. 1. displays the parameters of the Weibull analysis of different commercial and model basalt fibres. Depending on the type and the chemical composition of the natural resources, the processing conditions and the sizing, the variation of strength and modulus is rather extended. More details were pointed out in our previous work [1].

Considering the Weibull modulus as an indicator of fibre quality for different commercial fibres, COM4 and COM5 show a significantly enhanced performance. In comparison, Tab. 1 also reveals an overview of Weibull parameters of model fibres. MOD1 achieved a higher value of $\sigma_o$, however, the lower Weibull modulus *m* indicates an increased inhomogeneity of material.

The addition of $Al_2O_3$ (MOD3) leads to an improved mechanical performance compared to MOD1. Enhanced tensile strengths were also reported by Gutnikov et al. [4], who showed that an $Al_2O_3$-content increase of 10-24 wt% improved the strength almost 1.5-fold.

Tab. 1. Weibull parameters of commercial and model basalt fibres.

| | $\sigma_o$ [MPa] | m [-] | | $\sigma_o$ [MPa] | m [-] |
|---|---|---|---|---|---|
| **COM1** | 3472 | 7 | **MOD1** | 2921 | 5 |
| **COM2** | 1818 | 3 | **MOD2** | 2416 | 6 |
| **COM3** | 2659 | 7 | **MOD3** | 3026 | 6 |
| **COM4** | 3720 | 9 | **MOD4** | 3014 | 6 |
| **COM5** | 3474 | 9 | **MOD5** | 2681 | 6 |
| **COM6** | 2706 | 4 | | | |

Tab. 2. Calculated modulus of model basalt fibres within the strain range of 0-0,5%.

| | **Modulus [GPa]** |
|---|---|
| **MOD1** | 92±1 |
| **MOD2** | 84±1 |
| **MOD3** | 92±1 |
| **MOD4** | 92±0 |
| **MOD5** | 89±0 |

Tab. 2 shows the calculated modulus values of model basalt fibres according to equation 2. Similar to the tensile strength, MOD1 shows a higher modulus than MOD2, namely 92GPa and 84GPa, respectively.

The results show that alkali oxide act as a modifier in the glass network. The glass network seems to be more disordered. Lower bond strengths due to the breaking of Si-O-Si bonds led to a decreased stiffness of the fibre.

Modifying basalt MOD 1 by addition of $Al_2O_3$ (MOD3) as well as MgO (MOD4) shows in contrast to expectations no increasing effect. The calculated value remains 92 GPa. However, the addition of $TiO_2$ (MOD5) seems to be disadvantageous. The Weibull parameter $\sigma_o$ and *m* decrease related to performance of natural basalt MOD1.

### 3.2 Alkali resistance of model fibres

*Exposition in 3-ionic solution*

The failure stress distributions of MOD1 and MOD2 show, that ageing in 3-ionic solution leads to similarly corrosion behaviour like ageing in NaOH-solution. Firstly, failure stress distribution is shifted to smaller values, however with increased exposition time, e. g. 14 d as well as 28 d, failure stress increases again (Fig 3). A formation of a peeling shell was detected by SEM investigations of 28 d aged MOD1 fibres as well as MOD2 fibres.

If a peeling shell is detectable by SEM investigation, the corrosion process is very much advanced and it is very difficult to evaluate alkali resistance of model fibres by scale parameter $\sigma_o$, caused by an influence between the peeling off and the increased failure stress distribution like described in detail elsewhere [3].

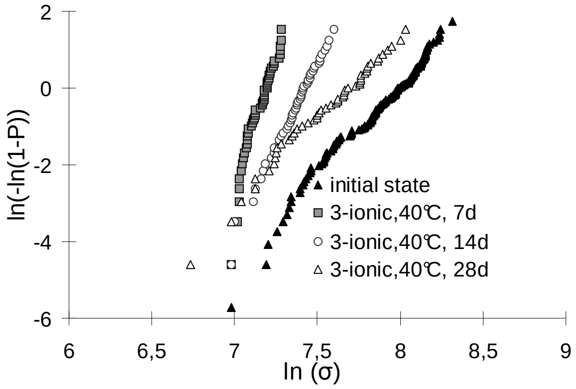


Fig. 3. Failure stress distribution of MOD1 after different exposition times in 3-ionic solution at 40°C.

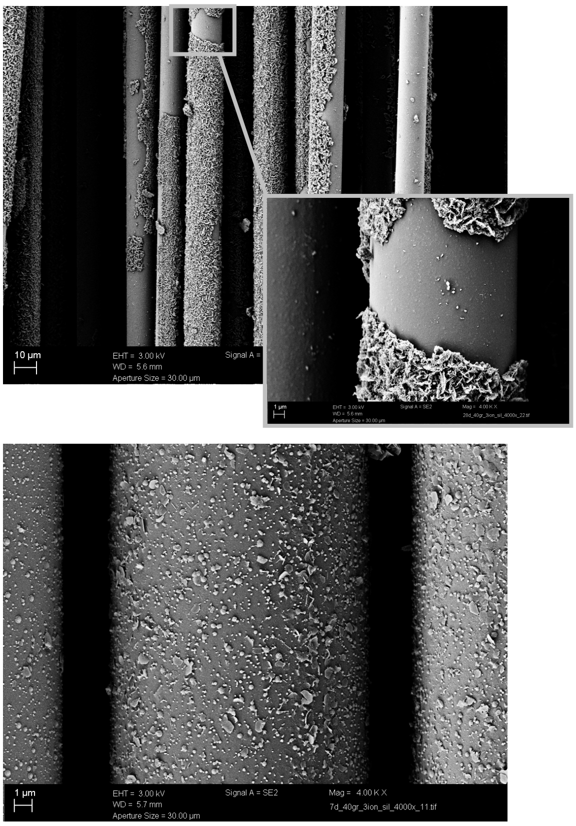

Fig. 4. SEM images of MOD 1 after treatment in 3-ionic solution at 40°C: 28 d (top); 7 d (bottom).

The SEM investigations of MOD1 (Fig. 4), as well as MOD2, fibre after 7d treatment reveal a strong attack of the fibre surface. However, the peeling-off-state has not been achieved, yet. After 7 d treatment, the scale parameter $\sigma_o$ of MOD 1 fibre is 1324 MPa and of MOD 2 fibre 1093 MPa. Related to initial values, the residual failure stresses are nearly the same value, namely 45 % and 43 %, respectively. That means an advantage of one of the compositions is not evident.

*Exposition in NaOH solution*

The formation of a peeling shell in NaOH solution was applied in another way to evaluate alkali resistance of model basalt fibres. Fig. 5 displays results of fibre diameter measurements after certain exposition time in NaOH solution at 80°C.

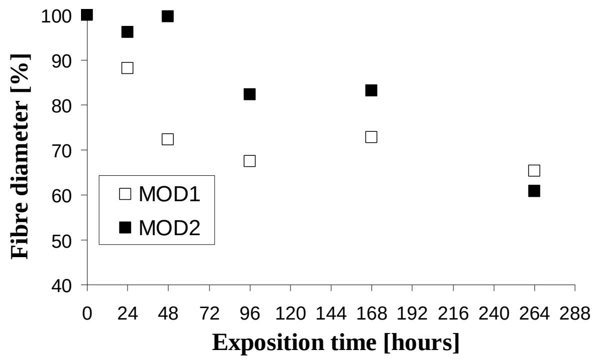


Fig. 5. Kinetic curves of alkali attack of model basalt fibres MOD1 and MOD2.

The dissolution of MOD1 starts rapidly in first 48h, whereas MOD2 seems to be resistant against alkali attack until 48h. Afterwards fibre diameter is also strongly reduced. However, the residual fiber diameter is still higher than that of MOD1 after 7d treatment. Reducing of fibre diameter of MOD 1 suggests a linear dissolution behaviour during 48h of alkaline attack, afterwards the generated corrosion layer seems to constrain the diffusion of alkaline media to the virgin surface and the dissolution of Si- network is slowed down. Estimated from the first linear dissolution behaviour a complete dissolution of fibre is expected after 7d. SEM images after 11 d treatment (Fig. 6) display a strongly developed peeling shell, but a residual fibre diameter still exists. After 11 d treatment in NaOH solution, both residual fibre diameters of MOD1 and MOD2 fibre are about 60%. MOD2 fibre cannot maintain the resistance against alkali attack permanently.

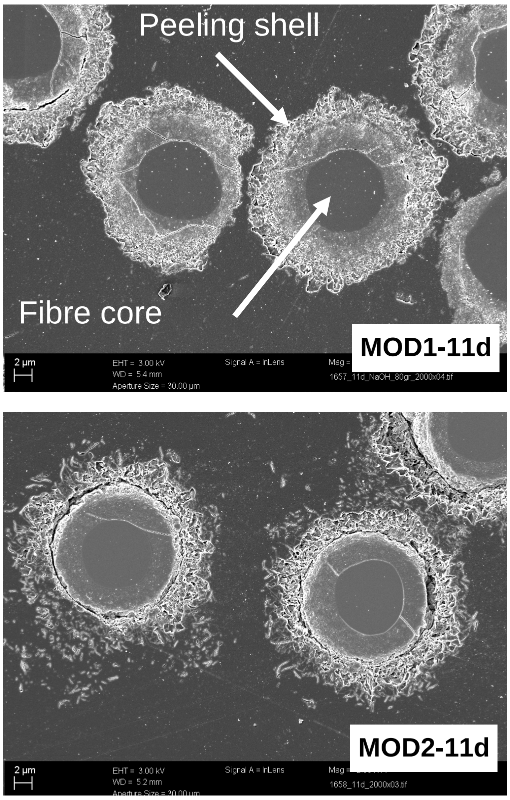


Fig. 6. SEM images of cross sections of MOD1 and MOD2 after 11d treatment in NaOH-solution at 80°C

The modification of chemical composition by additives led partly to an improvement of alkali resistance (Fig. 7). Both, MOD 3 and MOD 4 show an about 10 % increased residual fibre diameter after temperature accelerated treatment in NaOH solution. In contrast, the model basalt fibre MOD5 shows a more intensive formation of peeling shell. The residual fibre diameter of MOD 5 is probably smaller than 50 % after 4 d treatment in NaOH solution, caused by differentiation between corrosion layer and fibre core was not always unambiguous as distinguishable in Fig. 8.

It seems, that the addition of $TiO_2$ to MOD1 proved to be disadvantageous. The mechanical performance (Tab. 2, MOD 5) as well as alkali resistance was deteriorated for worse related to the initial chemical composition of MOD 1.

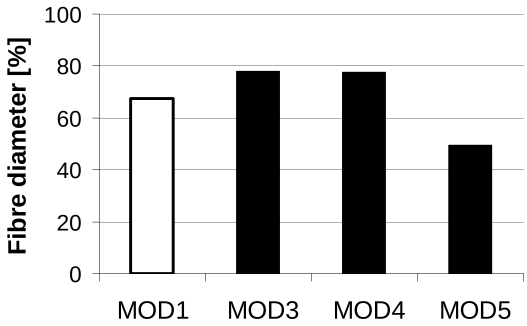


Fig. 7. Fibre diameter of model basalt fibres after 96 h exposition in 5% NaOH at 80°C.

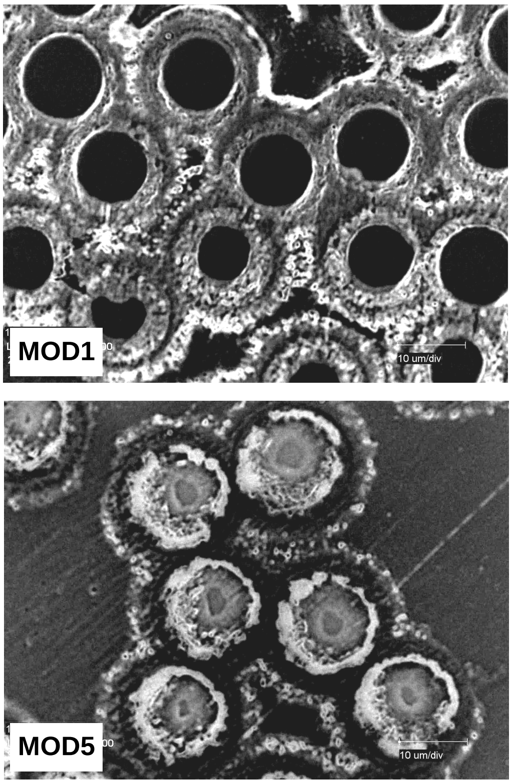


Fig. 8. Cross sections of MOD1 and MOD5 after ageing in 5 % NaOH at 80°C for 96h.

## 4 Conclusions

In this work the influence of chemical composition of basalt fibre properties like mechanical performance and alkali resistance was investigated.

Therefore, model basalt fibers were manufactured and evaluated by single fibre tensile tests and ageing tests in strong alkaline media. The results showed differences in performance of two natural basalt compositions. The one, which shows a worse mechanical performance, was identified temporarily advantageous in resistance against alkaline attack, and vice versa.
Modifying the basalt composition by adding $Al_2O_3$ or $MgO$ or $TiO_2$ revealed only moderate successful.
On the other hand $TiO_2$-addition was in general disadvantageous, whereas adding $Al_2O_3$ and $MgO$ increased tensile strength as well as alkali resistance in a positive way.

Furthermore, experiments showed that corrosion in 3-ionic solution leads to a similar corrosion behaviour like ageing in NaOH solution. A peeling shell is formed with progressive exposition time.
The formation of this shell is detectable by an increasing scale parameter of Weibull distribution. Therefore, the evaluation of alkali resistance by residual tensile strength is not advisable. In case of monofilaments, measuring the residual fibre diameter after alkali treatment is one possibility of a cross-check for evaluation of alkali resistance of fibres having different chemical compositions.

**Acknowledgements**

The authors wish to thank Dr. Jianwen Liu for experimental assistance and Dr. Christina Scheffler for helpful discussions.

References

[1] T. Förster, R. Plonka, C. Scheffler, E. Mäder „Challenges for fibre and interphase design of basalt fibre reinforced concrete" *RILEM Proc. pro075: Material Science – 2nd ICTRC –Textile Reinforced Concrete*, Theme 1, pp 57-66, 2010.

[2] J. Liu. Untersuchung von Verbundwerkstoffen mit Basalt- und PBO-Faser-Verstärkung. PhD thesis, TU Dresden, 2008

[3] C. Scheffler. T. Förster, E. Mäder, G. Heinrich, S. Hempel, V. Mechtcherine "Ageing of alkali-resistant glass and basalt fibres in alkaline solutions: Evaluation of the failure stress by Weibull distribution function "Journal of Non-Crystalline Solids", Vol. 355, 52-54, pp 2588-2595, 2009.

[4] S.I. Gutnikov, A.P. Malakho, B.I. Lazoryak and V.S. Loginov "Influence of Alumina on the properties of continous basalt fibres "*Russian Journal of inorganic chemistry*", Vol. 54, 2, pp 191-196, 2009.